

ROBUST DETECTION OF NUCLEAR QUADRUPOLE RESONANCE SIGNALS IN A NON-SHIELDED ENVIRONMENT

Tore Rudberg and Andreas Jakobsson

Dept. of Mathematical Statistics, Lund University, Sweden
Email: {tore, aj}@maths.lth.se

ABSTRACT

Nuclear quadrupole resonance (NQR) is a non-invasive radio-frequency technique allowing for a practically unique fingerprint for molecules containing quadrupolar nuclei, making the technique very promising for detection purposes. If properly excited, these nuclei will emit electromagnetic radiation, the frequency of which is governed mainly by where in the molecule the nuclei are positioned. However, the resulting NQR signals are inherently weak and are prone to strong interference signals from the measurement environment, making detection challenging. In this paper, we develop a robust and reliable detection algorithm that generalize earlier techniques and incorporates both efficient interference cancellation and the ability to handle multiple polymorphs in the sought substance. The usefulness of the algorithm is motivated by comparisons using realistic simulations.

1. INTRODUCTION

When exciting quadrupolar nuclei with properly selected radio frequency (RF) radiation, the resulting quadrupolar resonance yields a unique signal signature of the excited substance [1]. The technique can be used for detection of various harmful substances, such as explosives and drugs, as well as for the authentication of many forms of pharmaceutical substances. The ability to detect the former substances is clearly desired [2], but also the latter application is of significant importance [3]. Counterfeit medicines constitutes a dramatic problem in health care worldwide, and the problems are growing. According to the World Health Organization (WHO), counterfeit drugs constitute up to 25% of the total medicine supply in less developed countries. For instance, several forms of antimalarial medicines are commonly counterfeited, since these are expensive and the demand is high. In a study of antimalarial medicines from Cameroon in 2004, it was shown that 38% of the medicines marked Klorokin, 74% of those marked Kinin, and 12% of those marked Antifolates contained none or only trace amounts of the respective active substances [4]. Even in rich countries, WHO predicts that about 1% of all medicines are counterfeit. During recent years, a series of algorithms based on approximate maximum likelihood (AML) parameter estimation have been proposed for the detection of NQR signals [5–10], exploiting the detailed model for such signals developed in [6]. These techniques have also been extended to allow for multiple and/or polymorphic substances [7, 8], as well as for measurements made in a partly- or non-shielded environment [9, 10]. The ability to handle polymorphic and/or multiple substances

is of importance in the detection of several forms of high explosives, such as TNT, that occurs in both a monoclinic and an orthorhombic crystalline structure, and for many common pharmaceutical substances, where often only one of several possible crystalline structures acts as the active ingredient. In this work, we build on these earlier contributions, presenting a merged robust algorithm, termed RESPEQ (Robust Evaluation using Subspace-based methods of Polymorphic nuclei Ear Quadrupole signals), able to handle both polymorphic and/or multiple substances and the presence of very strong corrupting signals. The latter is typical in partly- or non-shielded measurement environments, commonly occurring for the mentioned applications of interest. To allow for efficient interference cancellation, the proposed algorithm assumes the availability of a primary data set, possibly containing the signal-of-interest (SOI), as well as a secondary SOI-free data set, only containing noise and interference signals. Such a secondary data set can, for echo train measurements, be obtained in-between the SOI measurements, while waiting for the nuclei to dephase to allow for further excitation (see also [9, 10]).

2. DATA MODEL

As described in [8], the m :th echo of an NQR signal from a pulse spin locking (PSL) sequence can be well modeled as

$$y_m(t) = \rho \sum_{p=1}^P \gamma_p y_m^{(p)}(t) + w_m(t), \quad (1)$$

where ρ , γ_p , $y_m^{(p)}(t)$, $w_m(t)$, and P are the overall gain, the relative proportion of the p :th polymorph, the signal from the p :th polymorph, additive noise, and the number of polymorphs, respectively. Furthermore, the proportions, $\{\gamma_p\}$, are defined such that $\sum_{p=1}^P \gamma_p = 1$, and [6]

$$y_m^{(p)}(t) = \sum_{k=1}^{d^{(p)}} \kappa_k^{(p)} e^{-(t+m\mu)\eta_k^{(p)}} e^{-\beta_k^{(p)}|t-t_{sp}|+i\omega_k^{(p)}(T)t}, \quad (2)$$

where, $t = t_0, \dots, t_{N-1}$, $m = 0, \dots, M-1$, t_{sp} , T , $d^{(p)}$, and μ are the echo sampling time, the echo number, the time between the (center of the) refocusing pulse and the echo center, the temperature, the number of sinusoidal components of the p :th polymorph, and the echo spacing, respectively. Moreover, $\kappa_k^{(p)}$, $\beta_k^{(p)}$, $\eta_k^{(p)}$, and $\omega_k^{(p)}(T)$ are the (complex) relative amplitude, the echo damping constant, the echo train damping constant, and the angular frequency of the k :th spectral line of the p :th polymorph. Typically, $t_0 \neq 0$ due to dead time in the measurement. It is also worth noting

This work was supported in part by the Swedish Research Council Carl Trygger's foundation, and the Wellcome trust.

that $\omega_k^{(p)}(T)$ is a known function of temperature, and that the number of polymorphs as well as the number of sinusoidal components of each polymorph are known. The relative amplitude vector $\boldsymbol{\kappa}$ is normalized so that for the p :th polymorph, $\max_k \{|\kappa_k^{(p)}|\} = 1$. Generally, $\boldsymbol{\kappa}$, $\boldsymbol{\beta}$, $\boldsymbol{\eta}$, and T can be assumed to be partially known, varying within a certain given interval [6]. The additive noise can be modeled as consisting of two parts. Firstly, the measurement will be corrupted by Johnson noise that can be well modeled as additive Gaussian white noise. However, this noise will be colored by the measurement equipment, causing a spectral shaping of the noise [5]. Secondly, the measurements are generally corrupted by substantial interference signals due to radio frequency interference (RFI), piezo-electric and/or magnetoacoustic responses. For simplicity, although somewhat incorrectly, we will here denote all these forms of interference signals as RFI. These forms of disturbances are modeled, for the m :th echo, as

$$w_m(t) = \mathcal{L}(\mathbf{G}\boldsymbol{\psi}_m + e_m(t)) \quad (3)$$

where \mathcal{L} , \mathbf{G} , $\boldsymbol{\psi}_m$, and $e_m(t)$ are the filter coloring the noise, a basis spanning the RFI subspace, the (complex) RFI weights, and a Gaussian white noise term, respectively. Note that the interference space, \mathbf{G} , is modeled as being the same for all echoes. For this to be a good model, the RFI needs to be close to stationary during the measurement.

In the following, let $(\cdot)^T$, $(\cdot)^*$, $(\cdot)^\dagger$, and $\|\cdot\|_2$ denotes the transpose, the conjugate transpose, the Moore-Penrose pseudo inverse, and the 2-norm, respectively.

3. ALGORITHM DERIVATION

As shown in [5], the coloring imposed by the measuring equipment, \mathcal{L} , can be well modeled as a low order autoregressive (AR) process. The prewhitening will therefore consist of passing the measured data through the corresponding inverse AR filter, \mathcal{L}^{-1} , as estimated from calibration data. In the model, this simply corresponds to a rescaling of the amplitudes of the spectral lines. Using (1) and (2), the m :th echo can be rewritten as [7]

$$\mathbf{y}_{Nm} \triangleq [y_m(t_0) \quad \dots \quad y_m(t_{N-1})]^T = \mathbf{D}_m \mathbf{g} + \mathbf{w}_N^m, \quad (4)$$

where

$$\mathbf{D}_m = \begin{bmatrix} \mathbf{A}_\theta^{(1)} \mathbf{B}_m^{(1)} & \dots & \mathbf{A}_\theta^{(p)} \mathbf{B}_m^{(p)} \end{bmatrix} \quad (5)$$

$$\mathbf{g} = \rho \begin{bmatrix} \gamma_1(\boldsymbol{\kappa}^{(1)})^T & \dots & \gamma_p(\boldsymbol{\kappa}^{(p)})^T \end{bmatrix}^T \quad (6)$$

with \mathbf{D}_m and \mathbf{g} being an $N \times \sum_{p=1}^P d^{(p)}$ matrix and a $\sum_{p=1}^P d^{(p)} \times 1$ vector, respectively,

$$\mathbf{A}_\theta^{(p)} = \begin{bmatrix} \mathcal{L}^{-1}(\lambda_1^{(p)})S_{1,t_0}^{(p)} & \dots & \mathcal{L}^{-1}(\lambda_{d^{(p)}}^{(p)})S_{d^{(p)},t_0}^{(p)} \\ \vdots & \ddots & \vdots \\ \mathcal{L}^{-1}(\lambda_1^{(p)})S_{1,\tilde{t}_{sp}}^{(p)} & \dots & \mathcal{L}^{-1}(\lambda_{d^{(p)}}^{(p)})S_{d^{(p)},\tilde{t}_{sp}}^{(p)} \\ \mathcal{L}^{-1}(\tilde{\lambda}_1^{(p)})S_{1,\tilde{t}_{sp}+1}^{(p)} & \dots & \mathcal{L}^{-1}(\tilde{\lambda}_{d^{(p)}}^{(p)})S_{d^{(p)},\tilde{t}_{sp}+1}^{(p)} \\ \vdots & \ddots & \vdots \\ \mathcal{L}^{-1}(\tilde{\lambda}_1^{(p)})S_{1,t_{N-1}}^{(p)} & \dots & \mathcal{L}^{-1}(\tilde{\lambda}_{d^{(p)}}^{(p)})S_{d^{(p)},t_{N-1}}^{(p)} \end{bmatrix}, \quad (7)$$

and $\mathbf{B}_m^{(p)}$ is a diagonal $d^{(p)} \times d^{(p)}$ matrix with diagonal elements $\begin{bmatrix} e^{-\eta_1^{(p)}m\mu} & \dots & e^{-\eta_{d^{(p)}}^{(p)}m\mu} \end{bmatrix}$. Furthermore,

$$S_{k,t}^{(p)} = e^{-\beta_k^{(p)}|t-t_{sp}|} e^{j\omega_k^{(p)}(T)t - \eta_k^{(p)}t}, \quad (8)$$

where \tilde{t}_{sp} is the latest time point such that $\tilde{t}_{sp} \leq t_{sp}$, and

$$\begin{cases} \lambda_k^{(p)} & = e^{j\omega_k^{(p)}(T) + \beta_k^{(p)} - \eta_k^{(p)}} \\ \tilde{\lambda}_k^{(p)} & = e^{j\omega_k^{(p)} - \beta_k^{(p)} - \eta_k^{(p)}} \end{cases} \quad (9)$$

The subscript θ for the \mathbf{A} matrix stresses the matrix's dependence of the unknown parameters of the p :th polymorph, $\boldsymbol{\theta}^{(p)}$, where

$$\boldsymbol{\theta}^{(p)} = [T \quad \boldsymbol{\beta}^{(p)} \quad \boldsymbol{\eta}^{(p)}]^T \quad (10)$$

$$\boldsymbol{\beta}^{(p)} = [\beta_1^{(p)} \quad \dots \quad \beta_{d^{(p)}}^{(p)}] \quad (11)$$

$$\boldsymbol{\eta}^{(p)} = [\eta_1^{(p)} \quad \dots \quad \eta_{d^{(p)}}^{(p)}] \quad (12)$$

Reminiscent of [10], the secondary data set is used to estimate the basis \mathbf{G} . This SOI-free data is prefiltered in the same way as above and then divided into blocks of the same length as the echoes, creating an $N \times K$ matrix \mathbf{Z}_{NK} , where each column is formed from one data block, and where K denotes the number of used blocks. Let

$$\mathbf{Z}_{NK} = \mathbf{U}\boldsymbol{\Sigma}\mathbf{V} \quad (13)$$

be the singular value decomposition (SVD) of \mathbf{Z}_{NK} , where \mathbf{U} and \mathbf{V} are unitary matrices containing the left and right singular vectors, respectively, and $\boldsymbol{\Sigma}$ is a diagonal matrix formed with the singular values of \mathbf{Z}_{NK} in non-increasing order on the main diagonal. The basis for the interference subspace is formed from the d_{int} most dominant (left) singular vectors, such that

$$\hat{\mathbf{G}} = [\mathbf{u}_1 \quad \mathbf{u}_2 \quad \dots \quad \mathbf{u}_{d_{int}}], \quad (14)$$

where \mathbf{u}_k is the k :th singular vector of \mathbf{U} , and d_{int} is selected using an MDL-based approach as detailed in [10]. As shown in [6], one may reduce the influence of interference signals by limiting the detector to be formed explicitly only from those frequency grid points where the frequencies of interest may occur. This is achieved by means of a frequency selective Fourier transform. By choosing a temperature interval that can be assumed to contain that of the sample, one may, using the temperature dependence of the resonance frequencies, determine the frequency ranges that may contain the spectral lines of interest [6]. Considering a set of frequency grid points in these narrow frequency bands, i.e.,

$$\left\{ \frac{2\pi k_1}{N}, \frac{2\pi k_2}{N}, \dots, \frac{2\pi k_L}{N} \right\} \quad (15)$$

where k_1, \dots, k_L are L integers corresponding to the (possibly overlapping) frequency grid points matching the possible ranges which may contain the SOI. Using (15), a frequency-selective Fourier transform matrix is formed as

$$\mathbf{V}_L = [\mathbf{v}_{k_1} \quad \dots \quad \mathbf{v}_{k_L}] \quad (16)$$

where

$$\mathbf{v}_{k_j} = [1 \quad e^{i2\pi k_j/N} \quad \dots \quad e^{i2\pi k_j(N-1)/N}]^T. \quad (17)$$

This has the effect that the parts of the frequency spectrum that does not contribute to the detection of the signal are discarded. As an additional benefit, the speed of the algorithm is improved as fewer data points are used to form the decision. Let \mathbf{Z}_{LM} denote the $LM \times 1$ data vector containing M echoes, each formed using L frequency grid points. The resulting data model can thus be written as

$$\mathbf{Z}_{LM} \triangleq \mathbf{H}_\theta \phi + \mathbf{E}_{LM} \quad (18)$$

$$\mathbf{H}_\theta = \begin{bmatrix} \mathbf{H}_\theta^{(1)} & \dots & \mathbf{H}_\theta^{(P)} \end{bmatrix} \quad (19)$$

$$\mathbf{H}_\theta^{(p)} = \begin{bmatrix} \mathbf{V}_L^* \mathbf{\Pi}_{\hat{\mathbf{G}}}^\perp \mathbf{A}_\theta^{(p)} \mathbf{B}_0^{(p)} \\ \vdots \\ \mathbf{V}_L^* \mathbf{\Pi}_{\hat{\mathbf{G}}}^\perp \mathbf{A}_\theta^{(p)} \mathbf{B}_{M-1}^{(p)} \end{bmatrix} \quad (20)$$

$$\phi = \rho [\gamma_1 (\boldsymbol{\kappa}^{(1)})^T \dots \gamma_P (\boldsymbol{\kappa}^{(P)})^T] \quad (21)$$

$$\boldsymbol{\kappa}^{(p)} = [\kappa_1^{(p)} \dots \kappa_{d^{(p)}}^{(p)}]^T, \quad (22)$$

where $\mathbf{\Pi}_{\hat{\mathbf{G}}}^\perp = \mathbf{I} - \hat{\mathbf{G}}\hat{\mathbf{G}}^T$. Using the resulting model, the detection criterion is formed as a generalized likelihood ratio test (GLRT), using the estimated parameters best describing the observed data. These are found as

$$\hat{\phi} = \arg \min_{\phi} \|\mathbf{H}_\theta \phi - \mathbf{Z}_{LM}\|_2^2 \quad \text{subj. to} \quad \|\boldsymbol{\kappa} - \boldsymbol{\kappa}_a\|_2^2 \leq \varepsilon \quad (23)$$

for each possible grid point θ , which can thus be assumed to be known in the minimization. Here, the minimization is formed to reflect that the relative amplitudes are only approximately known; one thus initially finds the amplitude vector $\boldsymbol{\kappa}$ that best describes the observations, given that this vector should be in the vicinity of the *a priori* assumed amplitude vector, $\boldsymbol{\kappa}_a$. The radius of the hypersphere, $\sqrt{\varepsilon}$, thus dictates the allowed deviation of the resulting estimate as compared to the prior information, and will depend on the uncertainty model of this deviation [8]. For the found amplitude vector, the remaining model parameters are found such that

$$\hat{\theta} = \arg \min_{\theta} \|\mathbf{H}_\theta \hat{\phi} - \mathbf{Z}_{LM}\|_2^2 \quad (24)$$

where $\hat{\phi}$ denotes the estimated amplitude vector as given by (23) for the grid point θ . The coupled minimizations can be solved as follows: Disregarding the constraint in (23), a solution may be found as

$$\hat{\phi} = \mathbf{H}_\theta^\dagger \mathbf{Z}_{LM} \triangleq (\mathbf{H}_\theta^* \mathbf{H}_\theta)^{-1} \mathbf{H}_\theta^* \mathbf{Z}_{LM} \quad (25)$$

Let $\hat{\phi}_k^{(p)}$ denote the value of $\hat{\phi}$ corresponding to the k :th component of the p :th polymorph and let $\mathbf{g} = [g_1 \dots g_P]$, where $g_p = \rho \gamma_p$. Given the used normalization, and that the proportions should sum to unity, the estimates $\hat{\boldsymbol{\kappa}}$, $\hat{\boldsymbol{\gamma}}$, and $\hat{\rho}$ can then be found as

$$\hat{g}_p = \max_k (\|\hat{\phi}_k^{(p)}\|_2^2) \quad (26)$$

$$\hat{\boldsymbol{\kappa}}_k^{(p)} = \frac{\hat{\phi}_k^{(p)}}{\hat{g}_p} \quad (27)$$

$$\hat{\rho} = \sum_{p=1}^P \hat{g}_p \quad (28)$$

$$\hat{\boldsymbol{\gamma}}_p = \frac{\hat{g}_p}{\hat{\rho}} \quad (29)$$

Thus, if this solution satisfies the constraint in (23), then this is the solution to the minimization problem. However, if it does not, the solution to (23) should instead be found on the hypersphere boundary. As proposed in [8], using $\hat{\rho}$ and $\hat{\boldsymbol{\gamma}}$ as initial estimates of ρ and $\boldsymbol{\gamma}$, robust estimates of $\boldsymbol{\kappa}$ can then be found by solving the minimization problem

$$\arg \min_{\boldsymbol{\kappa}} \|\mathbf{Q}\boldsymbol{\kappa} - \mathbf{Z}_{LM}\|_2^2 \quad \text{subj. to} \quad \|\boldsymbol{\kappa} - \boldsymbol{\kappa}_a\|_2^2 = \varepsilon, \quad (30)$$

where

$$\mathbf{Q} = \begin{bmatrix} \hat{g}_1 \mathbf{H}_\theta^{(1)} & \dots & \hat{g}_P \mathbf{H}_\theta^{(P)} \end{bmatrix} \quad (31)$$

As shown in [11], the minimization in (30) can be solved using the SVD along with the use of Lagrange multipliers (see also [12]). Using the so-obtained $\hat{\boldsymbol{\kappa}}$, a new, robust estimate of \mathbf{g} is found by solving the least squares problem

$$\check{\mathbf{g}} = \arg \min_{\mathbf{g}} \|\mathbf{R}_\theta \mathbf{g} - \mathbf{Z}_{LM}\|_2^2, \quad (32)$$

where

$$\mathbf{R}_\theta = \begin{bmatrix} \mathbf{H}_\theta^{(1)} \hat{\boldsymbol{\kappa}}^{(1)} & \dots & \mathbf{H}_\theta^{(P)} \hat{\boldsymbol{\kappa}}^{(P)} \end{bmatrix} \quad (33)$$

The real-valued solution to (32) is found as

$$\check{\mathbf{g}} = (\mathbf{R}_\theta^* \mathbf{R}_\theta + (\mathbf{R}_\theta^* \mathbf{R}_\theta)^T)^{-1} [(\mathbf{Z}_{LM}^* \mathbf{R}_\theta)^T + \mathbf{R}_\theta^* \mathbf{Z}_{LM}]. \quad (34)$$

From this estimate, the final estimate of ϕ can be found as

$$\hat{\phi} = [g_1 \boldsymbol{\kappa}^{(1)} \dots g_P \boldsymbol{\kappa}^{(P)}]^T. \quad (35)$$

Using this estimate, and the resulting estimate $\hat{\theta}$, given by (24), the test statistic is formed as

$$\xi(\mathbf{Z}_{LM}) = \frac{\|\mathbf{Z}_{LM}\|_2^2}{\|\mathbf{Z}_{LM} - \hat{\mathbf{Z}}_{LM}\|_2^2}, \quad (36)$$

where $\hat{\mathbf{Z}}_{LM} = [\mathbf{H}_\theta \hat{\phi}]_{\theta=\hat{\theta}}$. The sought substance is deemed present in the sample if and only if

$$\xi(\mathbf{Z}_{LM}) > \vartheta, \quad (37)$$

where ϑ is an empirically predetermined threshold value. Estimations of the proportions of the contained polymorphs, as well as the overall amplitude, can be obtained using (26), where ρ gives an indication of the quantity of the sought substance. Comparing the thus obtained detector with the REMIQS detector [8], one notes that the primary difference lies in the signal domain, which is here, as seen in (20) and similar to [9, 10], formed in a space orthogonal to the expected interference subspace. As a result, it is expected that

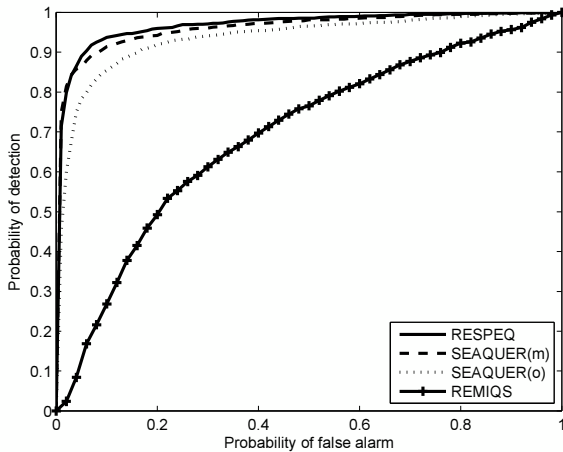


Figure 1: ROC curves for the RESPEQ, SEAQUER, and REMIQS algorithms, for SNR = -20 dB, ISR = 40dB.

the proposed RESPEQ detector will behave similar to the REMIQS detector for low levels of interference. Furthermore, if compared to the SEAQUER algorithm [9, 10], the proposed algorithm should allow for improved performance as the detection criterion in (36) is now formed as a combination of the contribution from the present polymorphs and compounds. Both these conclusions are confirmed in the following numerical study.

4. RESULTS

In this section, the performance of the proposed RESPEQ detector is compared to the earlier REMIQS and SEAQUER algorithms which it generalizes. To allow for easy comparison to the results in [8, 10], the algorithm is here evaluated on simulated TNT data containing both monoclinic and orthorhombic crystalline structures, but similar results are expected also on other similar substances. In the following, the interference to signal ratio (ISR) is defined as $\sigma_i^2 \sigma_s^{-2}$ and the signal to noise ratio (SNR) as $\sigma_s^2 \sigma_e^{-2}$, where σ_s^2 , σ_i^2 , and σ_e^2 are the power of the NQR signal, the RFI power, and the power of the noise without RFI, respectively. The RFI is simulated, using recorded radio transmissions, to resemble transmissions from three (amplitude modulated) radio stations with carrier frequencies close to the NQR frequencies of the sought substance. The necessary multidimensional grid search over θ is performed using a sequence of one-dimensional subsearches, which, as shown in [6, 13], only leads to a marginal loss of performance compared to a full grid search. In Figure 1, the ROC curves of the RESPEQ, SEAQUER, and REMIQS algorithms are shown, for a simulated NQR signal from a sample containing 50% monoclinic and 50% orthorhombic TNT, at a temperature of 285 K. In the figure, the ISR = 40 dB and the SNR = -20dB, and with the amplitudes having an additive truncated Gaussian error with variance σ^2 and uniformly distributed phase errors over $[-\phi, \phi]$, where $0 \leq \phi \leq 2\pi$. As in [8], to simplify presentation, this uncertainty is coupled in a uncertainty parameter, v , for both the phase and magnitude uncertainty as $\phi = \pi \frac{v}{100}$ and $\sigma^2 = 0.001v$. Here, v is set to 10%. As can be seen from

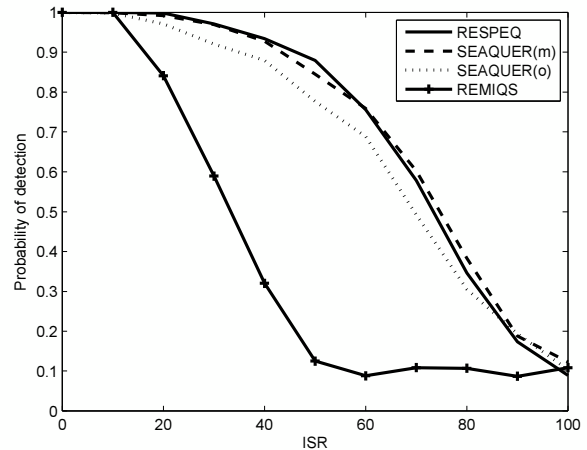


Figure 2: Probability of detection as a function of ISR, for $p_f = 10\%$, SNR = -20 dB.

the figure, the proposed RESPEQ algorithm clearly outperforms the REMIQS algorithm, but also the SEAQUER algorithm when tailored to detect the monoclinic and orthorhombic crystalline structures, respectively. These two tailored detectors are here termed SEAQUER(m) and SEAQUER(o) to stress which polymorph is targeted. The notable difference between the resulting detectors is due to the fact that the orthorhombic TNT signal has higher damping coefficients than the monoclinic, which has for effect that about two thirds of the (noise free) signal power originates from the monoclinic NQR signal. The plot is formed using 3000 Monte Carlo simulations. It is worth noting that the two here examined crystalline structures result in partly overlapping frequency components, thereby reducing the advantage of RESPEQ somewhat. For substances with better separated spectral support, one may expect the gain to be more noticeable. Figure 2 shows the impact of varying the RFI power, for a fixed probability of false alarm, $p_f = 0.1$. Apart from the ISR, the same parameters as above are used. Each point in the figure is calculated from 1000 Monte Carlo simulations. As noticeable from the figure, the performance of the REMIQS algorithm deteriorates quickly with increasing interference power, while the RESPEQ and the SEAQUER algorithms provides good detection even for very strong interference signals. An interesting observation is that the SEAQUER algorithm seems to be marginally less vulnerable to very strong RFI than RESPEQ. Note that in this plot, the RFI simulation is done in a more realistic way than in the corresponding plot in [10], making direct comparison misleading. Figure 3 and 4 show the mean square error (MSE) of the estimate of the proportion of monoclinic TNT as function of the ISR and uncertainty level, for SNR = 0dB. Figure 3 shows the impact of the uncertainty level, v , on the MSE of the estimation of the proportion of monoclinic TNT, γ_1 , for both the RESPEQ and the REMIQS algorithms, and for an ISR of 5dB and 25dB, respectively. For comparison, the Cramér-Rao lower bound (CRLB) for estimation of γ_1 without RFI is included in the plot (see also [8]). Since exact knowledge of the RFI is never available, no CRLB taking the RFI into account has been derived. As is apparent from

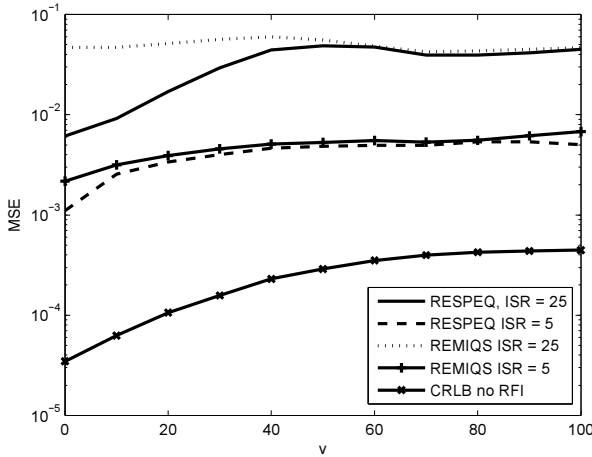


Figure 3: MSE of the estimated proportion of monoclinic TNT as a function of ν , for SNR = 0 dB and $\gamma = [0.6 \ 0.4]^T$.

the plot, the RESPEQ and REMIQS algorithms perform similarly for ISR = 5dB, although RESPEQ gives slightly better estimations. For ISR = 25dB, RESPEQ performs significantly better for low uncertainty, but the estimation collapses for higher uncertainty levels. In Figure 4, the MSE is instead shown as function of the ISR, for both algorithms and for $\nu = 5$ and $\nu = 30$, respectively. As expected, the REMIQS and the RESPEQ algorithms perform similarly for low ISR, whereas RESPEQ has an advantage for higher ISR values. For ISR higher than about 40, the algorithms are unable to estimate the proportions accurately.

5. ACKNOWLEDGEMENTS

The authors would like to thank Dr Erik Gudmundsson, Naveed R. Butt, and Stefan Adalbjörnsson at Lund University for useful discussions and assistance.

REFERENCES

[1] A. N. Garroway, M. L. Buess, J. B. Miller, B. H. Suits, A. D. Hibbs, A. G. Barrall, R. Matthews, and L. J. Burnett, "Remote Sensing by Nuclear Quadrupole Resonance," *IEEE Trans. Geoscience and Remote Sensing*, vol. 39, no. 6, pp. 1108–1118, June 2001.

[2] J. Miller and G. Barrall, "Explosives detection with nuclear quadrupole resonance," *American Scientist*, vol. 93, 2005.

[3] J. Harris, P. Stevens, and J. Morris, "Keeping it real - combating the spread of fake drugs in poor countries," Tech. Rep., International Policy Network, 2009.

[4] L. K. Basco, "Molecular epidemiology of malaria in cameroon xix. quality of antimalarial drugs used for self-medication," *American Journal of Tropical Medical Hygiene*, vol. 70, pp. 245–250, 2004.

[5] A. Jakobsson, M. Mossberg, M. Rowe, and J. A. S. Smith, "Exploiting Temperature Dependency in the Detection of NQR Signals," *IEEE Transactions on Signal Processing*, vol. 54, no. 5, pp. 1610–1616, May 2006.

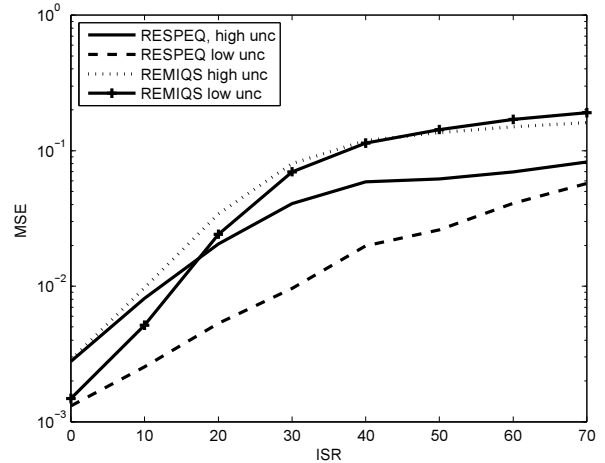


Figure 4: MSE of the estimated proportion of monoclinic TNT as a function of the ISR, for SNR = 0 dB and $\gamma = [0.6 \ 0.4]^T$.

[6] S. D. Somasundaram, A. Jakobsson, J. A. S. Smith, and K. Althoefer, "Exploiting Spin Echo Decay in the Detection of Nuclear Quadrupole Resonance Signals," *IEEE Trans. Geoscience and Remote Sensing*, vol. 45, no. 4, pp. 925–933, April 2007.

[7] S. D. Somasundaram, A. Jakobsson, and J. A. S. Smith, "Analysis of Nuclear Quadrupole Resonance Signals from Mixtures," *Signal Processing*, vol. 88, no. 1, pp. 146–157, January 2008.

[8] N. R. Butt, S. D. Somasundaram, A. Jakobsson, and J. A. S. Smith, "Frequency-Selective Robust Detection and Estimation of Polymorphic QR Signals," *Signal Processing*, vol. 88, no. 4, pp. 834–843, April 2008.

[9] S. D. Somasundaram, A. Jakobsson, M. D. Rowe, J. A. S. Smith, N. R. Butt, and K. Althoefer, "Robust Detection of Stochastic Nuclear Quadrupole Resonance Signals," *IEEE Transactions on Signal Processing*, vol. 56, no. 9, pp. 4221–4229, September 2008.

[10] S. D. Somasundaram, A. Jakobsson, and N. R. Butt, "Countering Radio Frequency Interference in Single-Sensor Quadrupole Resonance," *IEEE Geoscience and Remote Sensing Letters*, vol. 6, no. 1, pp. 62–66, Jan. 2009.

[11] G. H. Golub and C. F. Van Loan, *Matrix Computations*, The John Hopkins University Press, 3rd edition, 1996.

[12] S. D. Somasundaram, A. Jakobsson, and E. Gudmundsson, "Robust Nuclear Quadrupole Resonance Signal Detection Allowing for Amplitude Uncertainties," *IEEE Trans. Signal Processing*, vol. 56, no. 3, pp. 887–894, March 2008.

[13] S. D. Somasundaram, *Advanced Signal Processing Algorithms Based on Novel Nuclear Quadrupole Resonance Models for the Detection of Explosives*, Ph.D. thesis, King's College London, London, United Kingdom, 2007.